The Nature of Predictability Enhancement in a Low-Order Ocean–Atmosphere Model

JON M. NESE

Department of Environmental Sciences, The Pennsylvania State University, Hazleton, Pennsylvania

ARTHUR J. MILLER

Scripps Institution of Oceanography, La Jolla, California

JOHN A. DUTTON

Department of Meteorology, The Pennsylvania State University, University Park, Pennsylvania

(Manuscript received 1 September 1995, in final form 7 March 1996)

ABSTRACT

A low-order moist general circulation model of the coupled ocean–atmosphere system is reexamined to determine the source of short-term predictability enhancement that occurs when an oceanic circulation is activated. The predictability enhancement is found to originate predominantly in thermodynamic processes involving changes in the mean hydrologic cycle of the model, which arise because the mean sea surface temperature is altered by the oceanic circulation. Thus, time-dependent sea surface temperature anomalies forced by anomalous geostrophic currents in the altered mean conditions do not contribute to the dominant ocean–atmosphere feedback mechanism that causes the predictability enhancement in the model.

1. Introduction

The predictability time scales of two low-order coupled midlatitude ocean–atmosphere models were compared using measures from dynamical systems theory in Nese and Dutton (1993, hereafter referred to as ND93). In the first model (based on Lorenz 1984), a baroclinic, quasigeostrophic atmosphere is coupled to a thermodynamic ocean that generates sea surface temperature variations driven solely by surface heat fluxes (termed the "inert" ocean case in ND93). In the second model, ND93 allow an oceanic circulation driven by atmospheric wind stress to develop (the "active" ocean case). One conclusion of ND93 was that allowing the simple gyrelike oceanic circulation to be driven by the atmospheric model delivers about a 15% enhancement to the average error doubling time of the atmosphere, compared to the same ocean–atmosphere model with only air–sea heat fluxes.

It was intriguing to find such a considerable increase in the predictability time scale of the coupled midlatitude system because ocean currents were apparently responsible for the enhancement. One would have expected ocean currents to only weakly affect the predictability time scales of the basic coupled model case since it is generally acknowledged that air–sea heat fluxes dominate the generation of SST anomalies in the real midlatitude ocean (e.g., Cayan 1992).

We have extended the analyses of ND93 and have thereby addressed the following questions in this paper. First, which mechanisms in the model are responsible for the predictability enhancement that occurs in the active ocean case? For example, is the predictability enhancement tied to midlatitude ocean–atmosphere feedback involving SST anomalies? Second, to what extent is the predictability enhancement identified in the model realistic, and what do the model results suggest about predictability enhancement in the actual ocean–atmosphere system?

2. Persistence and predictability

Qualitatively, one might expect a thermodynamically coupled ocean–atmosphere model to generate thermal inertia that would enhance the predictability of the system, compared to an uncoupled model. ND93 proposed that additional dynamic (as opposed to thermal) inertia might be responsible for the predictability enhancement in the active ocean case when they stated that "if a circulation is permitted to develop in the model ocean, then the additional inertia in the system might further enhance predictability, in analogy with a flywheel." In this section, we present new results on quantifying these changes in persistence and predict-

Corresponding author address: Dr. Jon M. Nese, The Pennsylvania State University, 108 Kostos Bldg., Highacres, Hazleton, PA 18201.
E-mail: j2n@psuvm.psu.edu

ability time scales (as defined in ND93) and identifying the physics behind them.

In ND93, atmosphere–ocean states in the active ocean case were shown to be more persistent, on average, than those in the inert ocean case (see Fig. 5 of ND93). The persistence measure $C(t)$ used in ND93 is essentially a measure of phase space velocity; this measure can be analyzed to determine the contribution of each prognostic variable (atmospheric streamfunction Ψ, atmospheric temperature T, atmospheric total dewpoint W, and oceanic temperature S) to the difference in persistence between the inert and active ocean cases. These new calculations reveal that the atmospheric moisture variable W accounts for nearly two-thirds of the decrease in phase space velocity that occurs when the oceanic circulation is activated. Thus, differences in the hydrologic cycles in the models are responsible for most of the increase in persistence in the active ocean case.

In ND93, average predictability was expressed in terms of Lyapunov exponents, which measure the divergence of adjacent trajectories in a phase space having as many dimensions as there are spectral coefficients in the model. The largest Lyapunov exponent was 0.062 bits day^{-1} in the inert ocean case (corresponding to an average error doubling time of about 16 days) and 0.052 bits day^{-1} in the active ocean case (corresponding to an average error doubling time of about 19 days). The enhancement in predictability quantified by the difference in the largest Lyapunov exponent between the two cases [0.010 bits day^{-1} $= -(0.052 - 0.062)$ bits day^{-1}] represents a reduction in the average divergence of adjacent trajectories in phase space; that is, the perturbation vector identified with the largest Lyapunov exponent grows at a smaller average rate in the active ocean case than in the inert ocean case.

Because the length of the perturbation vector is the square root of the sum of the squares of each component (and each component corresponds to a spectral coefficient), the contribution of each spectral coefficient to the length of the perturbation vector can be estimated at each time step using a linear differential analysis. For each component, an average of its contribution was computed over all time steps in which the sum of the contributions (as derived from the linear differential analysis) was within 5% of the actual length of the perturbation vector. This procedure was performed for both the inert and active ocean cases, and the results were compared to determine the contribution of each spectral coefficient (and thus each prognostic variable) to the predictability enhancement in the active ocean case. These contributions are given in Table 1.

These results show that most of the predictability enhancement in the active ocean case occurs in the atmospheric moisture variable W. Additional predictability enhancement, almost half that attributable to W,

occurs in the atmospheric streamfunction Ψ, while atmospheric temperature contributes minimally to the enhanced predictability of the system. The negative value for oceanic temperature S indicates that oceanic temperature is actually less predictable in the active ocean case. Thus, although predictability in the complete coupled ocean–atmosphere system is enhanced in the active ocean case, oceanic temperature is less predictable.

To examine the predictability results obtained in the form of Lyapunov exponents, we have computed the standard anomaly correlation coefficient for Ψ, T, W, and S for a 2-yr prediction period. A 1000-yr climatological integration was run for both the inert and active ocean cases. Every 20 years during these climatological runs, the spectral coefficients were perturbed. The perturbations were not random, but rather in the direction in phase space corresponding to the local divergence rate whose average is the largest Lyapunov exponent. In magnitude, the resultant amplitude of the perturbation in the height field was 2-m global rms and in the T, W, and S fields 0.5°C global rms. The perturbed initialized fields were then integrated forward for 2 years. Thus, the ensemble of cases consists of 50 2-yr control (climatological) and perturbed integrations.

The ensemble means of the anomaly correlation measure for Ψ, T, W, and S for the inert and active ocean cases, shown in Fig. 1, confirm the Lyapunov exponent results: atmospheric total dewpoint, atmospheric streamfunction, and atmospheric temperature are more predictable in the active ocean case, while oceanic temperature is more predictable in the inert ocean case.

Because predictability enhancement in the model is linked to changes in the moisture field in the model, a few comments concerning the simplified representation of moisture in the model are appropriate. In an attempt to circumvent difficulties typically associated with a spectrally truncated representation of the radiative and thermodynamic processes in a moist atmosphere, Lorenz (1984) chose that the prognostic moisture variable in the model would represent total water content, not water vapor content; Lorenz (1984) calls this variable "total dewpoint," defined as the value the dewpoint would acquire if all the liquid water were converted to vapor. A diagnostic equation is used to specify how much of the total water is vapor and how much is liquid. The underlying ocean exchanges water with the atmosphere through simplified representations of precipitation and evaporation; the exchanges are proportional to differences between the atmospheric water vapor mixing ratio and mixing ratios based on W and S. The extent to which this simplified and somewhat unique approach to the representation of a moist atmosphere is responsible for the predictability enhancement is not addressed here and remains to be explored.

TABLE 1. Distribution of predictability enhancement (in bits day^{-1}) in the active ocean case among the individual spectral coefficients (positive value indicates enhanced predictability in the active ocean case). The total enhancement is approximately 0.01 bits day^{-1}; that is, the largest Lyapunov exponent in the active ocean case is 0.01 bits day^{-1} less than in the inert ocean case.

Ψ_1	0.001930	W_0	0.000087	T_0	−0.000016	S_0	−0.000001
Ψ_2	0.001005	W_1	−0.000745	T_1	0.001389	S_1	−0.000661
Ψ_3	0.000095	W_2	0.006854	T_2	0.000606	S_2	−0.000852
Ψ_4	−0.000075	W_3	0.000130	T_3	−0.000117	S_3	−0.000090
Ψ_5	0.000159	W_4	0.000768	T_4	−0.000666	S_4	−0.000050
Ψ_6	0.000857	W_5	0.001135	T_5	−0.000209	S_5	−0.000002
		W_6	−0.001122	T_6	−0.000381	S_6	−0.000004
	0.003971		0.007107		0.000606		−0.001660

3. The role of SST anomalies and changes in mean SST

We next inquire whether the addition of an oceanic circulation affects variable surface heat fluxes (via altered SST anomalies) to produce the enhancement in predictability, and/or whether a shift in the mean heat flux (via an altered mean SST) is somehow responsible. Note that the representations of the exchanges of sensible and latent heat across the ocean–atmosphere interface are similar to those used for the exchanges of water. Briefly, these fluxes are proportional to the differences of the appropriate quantities across the interface, with the same factor of proportionality k used for all exchanges. A time constant of 5 days was chosen as the value of $1/k$.

The ocean circulation model in ND93 is the rigid-lid barotropic vorticity equation for a single constant depth layer [cf. Pedlosky (1975), who invoked a similar model of ocean current advection]. In this model, mean and fluctuating geostrophic currents are calculated as a function of space and time, driven by the curl of the atmospheric wind stress. Since the low-order ocean model has a rigid lid, the oceanic vorticity waves occur as fast barotropic waves with basin scale. These barotropic waves have never been shown to generate SST anomalies in the real ocean, and, considering the fast time scales (a few days) and small velocities (a few mm s^{-1}) associated with observed fluctuating open-ocean geostrophic barotropic currents, it is unlikely that such currents could be capable of doing so, particularly over time scales of weeks. In the model, however, the rms amplitude of SST variability increases from 0.25°C in the inert ocean case to 0.36°C in the active ocean case. In spite of this increase, the results discussed in section 2 indicate that time-dependent SST anomalies (and the associated ocean–atmosphere feedback) do not play a substantial role in the predictability enhancement that occurs in the active ocean case of ND93. Indeed, the SST anomalies themselves are less predictable in the presence of these geostrophic currents than their solely heat-flux-forced analogues (Table 1).

In contrast, it is evident that the shift in the mean model SST (Figs. 2d and 4 in ND93) and the commensurate shift in atmospheric surface temperature (Fig. 6 in ND93) are tied to the increase in predictive time scale. The decrease in the north–south atmospheric thermal gradient (Fig. 6 in ND93) reflects a reduced mean potential energy upon which the atmospheric transients may feed. In addition, the more persistent atmospheric flows in the active ocean case, when interpreted in light of the change in the mean SST (that is, the undulation that appears in the average SST field in the active ocean case), suggest that a type of "thermal anchoring" is occurring in the model in the active ocean case, an analogy of how real atmospheric waves are anchored by topography and land–ocean boundaries. However, the undulations in mean ocean surface isotherms seen in the active ocean case are somewhat exaggerated compared to reality, so the effect of this anchoring on predictability in the model is also likely somewhat exaggerated.

4. Effect of a model alteration

As this manuscript was in progress, the authors became aware (A. Fournier 1995, personal communication) that an error had been discovered in the original model code used by Lorenz (1984) and subsequently ND93. The discrepancy involves a factor of $1 + \lambda$ in one coefficient of the spectral form of one of the differential equations, in which λ is the static stability parameter in the model. With the revised code, the inert ocean case in ND93 (which is Lorenz's original model) no longer exhibits chaotic behavior at Lorenz's reference parameters of $\lambda = 0.2$ and $T_0^* = 273$ K (T_0^* specifies the magnitude of the globally averaged solar forcing in the model).

Stewart (1996) has determined that one effect of revising the model code is to shift the chaotic regime of the model to larger values of the static stability parameter. He reports that chaotic behavior occurs in the revised model for $\lambda = 0.215$ and values of T_0^* near 276.5. We found that choosing $\lambda = 0.215$ and $T_0^* = 276.4$ yields chaotic solutions with globally averaged air and ocean temperatures of the same magnitude (about 288 K) and variabilities as those found in the simulations reported in ND93. Thus, to determine whether our predictability results are robust under this model alteration, we chose these values of λ and T_0^*, and recalculated the Lyapunov exponents in both the inert and active ocean cases.
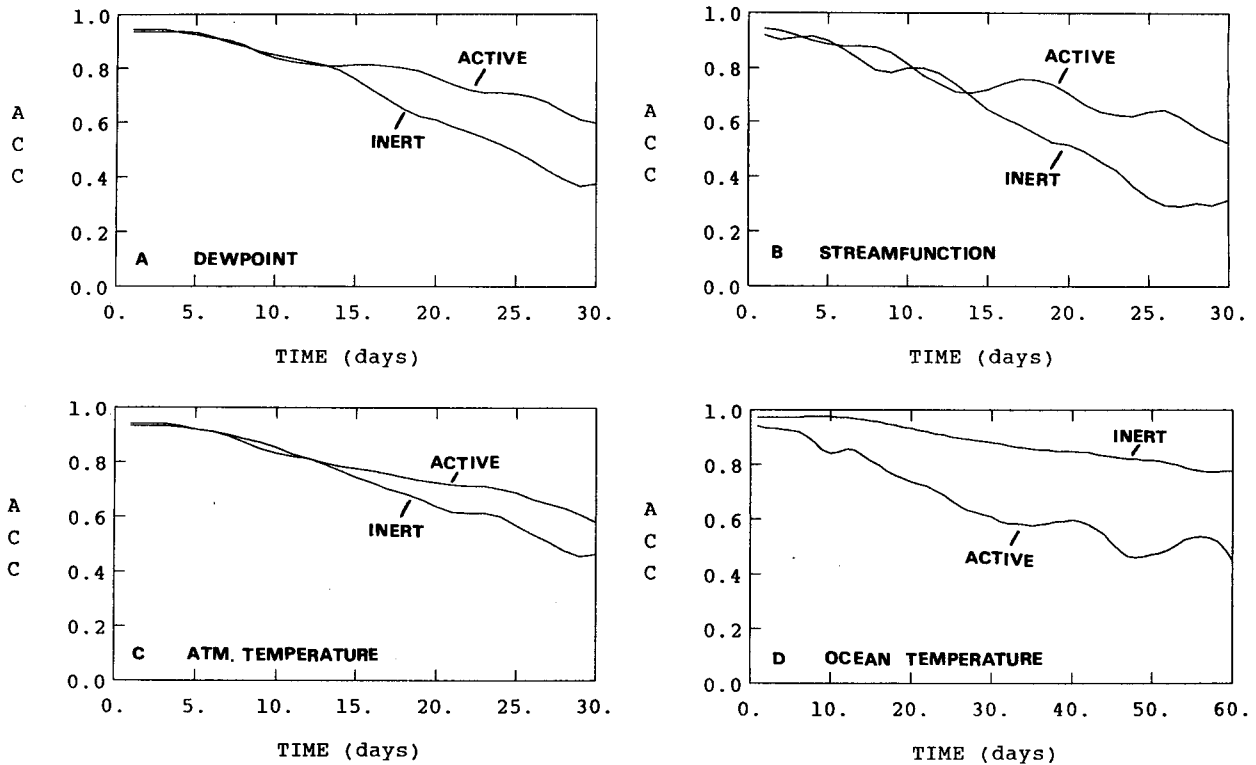
FIG. 1. Ensemble mean of anomaly correlation coefficient for (a) atmospheric total dewpoint W, (b) atmospheric streamfunction Ψ, (c) atmospheric temperature T, and (d) oceanic temperature S.

The nine largest Lyapunov exponents of the revised model are given in Table 2 (for comparison, the nine largest Lyapunov exponents for the inert and active ocean cases using the original code are repeated from ND93). Once again, predictability is enhanced when the oceanic circulation is activated, although the enhancement is greater than in the original model of ND93. We then recomputed the contribution of each spectral coefficient to the predictability enhancement. Table 3 is like Table 1, but for the revised code. Comparing Tables 1 and 3 shows that even after the model alteration, the moisture variable W dominates the predictability enhancement once the oceanic circulation is activated, while the atmospheric streamfunction is second in importance. Again, atmospheric temperature also contributes minimally to predictability enhancement in the revised code. Oceanic temperature, as in the original model, is less predictable once the oceanic circulation is activated.

To evaluate the robustness of these results with respect to variations in the solar forcing, we repeated these predictability experiments for both the inert and active ocean cases using $\lambda = 0.215$ and values of T_0^* of 276, 276.25, and 276.5 (these values of the globally averaged solar forcing produce chaotic solutions with globally averaged atmospheric temperatures of approx-

imately 280, 285, and 290 K, respectively). For all these choices of T_0^*, the active ocean case is more predictable, with the enhancement ranging from a minimum of 10% for $T_0^* = 276$ to a maximum of 75% for $T_0^* = 276.5$. Thus, we conclude that the predictability enhancement in the revised model is robust at realistic choices of the solar forcing parameter.

5. Concluding remarks

In ND93, techniques were introduced for quantifying predictability in models of the climate system. These techniques were applied to a pair of low-order ocean–atmosphere models to demonstrate that the predictability of a coupled model is enhanced when an atmospherically driven oceanic circulation is permitted to develop.

We conclude that, in this model, the increased predictability of the active ocean case is generated predominantly by thermodynamic processes involving the hydrologic cycle, which arise because the mean SST is altered by the oceanic circulation. The wavelike structure of the mean SST field in the active ocean case provides a boundary condition with spatial variations that slow both the growth of perturbations and the phase space velocities of the variables, creating a more

TABLE 2. The nine largest Lyapunov exponents of the inert and active ocean cases for the original code used in ND93 and the revised code. Units are bits day^{-1}.

	Original code		Revised code	
	Inert	Active	Inert	Active
γ_1	0.062	0.052	0.073	0.046
γ_2	0.004	0.005	0.006	0.001
γ_3	0.000	0.000	0.000	0.000
γ_4	−0.002	−0.006	−0.004	−0.009
γ_5	−0.010	−0.015	−0.025	−0.031
γ_6	−0.022	−0.028	−0.037	−0.045
γ_7	−0.032	−0.035	−0.045	−0.057
γ_8	−0.041	−0.041	−0.050	−0.070
γ_9	−0.052	−0.053	−0.060	−0.085

predictable atmosphere as well as a more predictable ocean–atmosphere system and, surprisingly, a more chaotic SST. Increased persistence of atmospheric flows in the active ocean case, probably as a result of enhanced thermal anchoring of atmospheric waves, suggests that the wavy structure of the mean model SST in the active ocean case is directly linked to the change in predictive time scale.

Because the prognostic variable responsible for most of the predictability enhancement is atmospheric total dewpoint, one must ask whether the enhancement is an artifact of the simplified formulation of moisture in the model. It is unclear whether better-resolved models, with more realistic moisture and oceanic circulation representations, will exhibit a similar predictability enhancement.

The effects of anomalous geostrophic current advection on midlatitude SST anomalies and subsequent ocean–atmosphere feedback were not the dominant cause of predictability enhancement in the model of ND93 over time scales of a few weeks. Indeed, geostrophic current anomalies acting on the SST are unlikely to be an important oceanic mechanism for altering air–sea thermal feedback, though oceanic vertical mixing variations and large-scale Ekman current advection may be (cf. Frankignoul 1985). Thus, although the simple system discussed in ND93 is interesting in its own right, and although the atmospheric and oceanic

patterns in the model agree (qualitatively and somewhat quantitatively) with observations of the actual ocean–atmosphere system, the applicability of the results regarding predictability must be kept in perspective when considering the real ocean–atmosphere system.

Though time-dependent midlatitude SST anomalies fail to exhibit a dominant effect on enhancing predictability of the ocean–atmosphere system in the simple model of ND93, an important effect of gyre-scale circulation is nonetheless made manifest in the results, particularly with respect to annual and longer time scales. Since the mean SST field is partly controlled by the presence of large-scale oceanic gyres, in both this model and in nature, the model results show that changes in gyre-scale oceanic flows can result in significant changes in the atmospheric hydrologic cycle and, hence, the atmospheric climate. Large-scale changes in wind-forced oceanic gyres have been diagnosed in the Atlantic and Pacific Oceans over interannual time scales (Sekine 1988; Trenberth 1991; Greatbatch et al. 1991; Miller et al. 1996), and the ND93 model results suggest that the surface signature of these geostrophic circulation changes may couple back to large-scale atmospheric circulation regime changes through ocean–atmosphere feedback on the gyre scale. By using the dynamical systems diagnostic techniques of ND93, one is able to follow the influence of mean SST changes on the water cycle and eventually on the mean atmospheric state and its resultant intrinsic variability on weekly and annual time scales.

The use of simplified coupled ocean–atmosphere models, such as the one explored here, is essential for unraveling the complexities of short-term coupled interactions in the midlatitudes. Studies of these mechanisms have invoked systems ranging from the low-order models of Palmer (1993) and Lorenz (1984) through the moderate complexity models of Salmon and Hendershott (1976), Roads (1989), Miller and Roads (1990), Phillips (1992), Alexander (1992a,b), Gallimore (1995), and Tokioka et al. (1992). All the models simplify some aspects of the feedback mechanisms of the complete coupled ocean–atmosphere system. It is important when discussing and analyzing such

TABLE 3. Distribution of predictability enhancement (in bits day^{-1}) in the active ocean case among the individual spectral coefficients (positive value indicates enhanced predictability in the active ocean case) for the revised model. The total enhancement is about 0.026 bits day^{-1}.

		W_0	0.000767	T_0	0.000037	S_0	−0.000001
Ψ_1	0.003155	W_1	0.007178	T_1	0.001665	S_1	−0.000300
Ψ_2	0.002306	W_2	0.006818	T_2	0.002072	S_2	−0.000912
Ψ_3	0.000153	W_3	0.000809	T_3	0.000118	S_3	−0.000021
Ψ_4	0.000204	W_4	0.001033	T_4	−0.000461	S_4	−0.000136
Ψ_5	0.000164	W_5	0.000830	T_5	−0.000245	S_5	−0.000055
Ψ_6	0.001117	W_6	0.000411	T_6	−0.000042	S_6	−0.000022
	0.007099		0.017846		0.003144		−0.001447

models to identify as clearly as possible the mechanisms that cause the effects that are exposed by the analyses, as the dynamical systems approach of ND93 is capable of doing.

REFERENCES

Alexander, M. A., 1992a: Midlatitude atmosphere–ocean interaction during El Niño. Part I: The North Pacific Ocean. *J. Climate,* **5,** 944–958.
——, 1992b: Midlatitude atmosphere–ocean interaction during El Niño. Part II: The Northern Hemisphere Atmosphere. *J. Climate,* **5,** 959–972.
Cayan, D. R., 1992: Latent and sensible heat flux anomalies over the northern oceans: Driving the sea surface temperature. *J. Phys. Oceanogr.,* **22,** 859–881.
Frankignoul, C., 1985: Sea surface temperature anomalies, planetary waves, and air–sea feedback in the middle latitudes. *Rev. Geophys.,* **23,** 357–390.
Gallimore, R. G., 1995: Simulated ocean–atmosphere interaction in the North Pacific from a GCM coupled to a constant-depth mixed layer. *J. Climate,* **8,** 1721–1737.
Greatbatch, R. J., A. F. Fanning, A. D. Goulding, and S. Levitus, 1991: A diagnosis of interpentadal circulation changes in the North Atlantic. *J. Geophys. Res.,* **96,** 22 009–22 023.
Lorenz, E. N., 1984: Formulation of a low-order model of a moist general circulation. *J. Atmos. Sci.,* **41,** 1933–1945.
Miller, A. J., and J. O. Roads, 1990: A simplified coupled model of extended range predictability. *J. Climate,* **3,** 523–542.

——, D. R. Cayan, and W. B. White, 1996: A decadal change in the North Pacific thermocline and gyre-scale circulation. *J. Climate,* in press.
Nese, J. M., and J. A. Dutton, 1993: Quantifying predictability variations in a low-order ocean–atmosphere model: A dynamical systems approach. *J. Climate,* **6,** 185–204.
Palmer, T. N., 1993: Extended range atmospheric prediction and the Lorenz model. *Bull. Amer. Met. Soc.,* **74,** 49–65.
Pedlosky, J., 1975: The development of thermal anomalies in a coupled ocean–atmosphere model. *J. Atmos. Sci.,* **32,** 1501–1514.
Phillips, T. J., 1992: An application of a simple coupled ocean–atmosphere model to the study of seasonal climate prediction. *J. Climate,* **5,** 1078–1096.
Roads, J. O., 1989: Linear and nonlinear responses to middle latitude temperature anomalies. *J. Climate,* **2,** 1014–1046.
Salmon, R., and M. C. Hendershott, 1976: Large-scale air–sea interactions with a simplified general circulation model. *Tellus,* **28,** 228–242.
Sekine, Y., 1988: Anomalous southward intrusion of the Oyashio east of Japan. I. Influence of the interannual and seasonal variations in the wind stress over the North Pacific. *J. Geophys. Res.,* **93,** 2247–2255.
Stewart, H. B., 1996: The Lorenz low-order moist atmospheric circulation model: Regimes and bifurcations. (Unpublished manuscript), 30 pp. [Available from Department of Applied Science, Brookhaven National Laboratory, Upton, NY 11173.]
Tokioka, T., A. Kitoh, and S. Nakagawa, 1992: Relationships between monthly mean sea surface temperature anomalies and sea level pressure anomalies realized in a coupled atmosphere–ocean general circulation model. *Second Int. Conf. on Modelling Global Climate Change and Variability,* Hamburg, Germany, Max-Planck-Institute for Meteorology, p. 54.
Trenberth, K., 1991: Recent climate changes in the Northern Hemisphere. *Greenhouse-Gas Induced Climate Change: A Critical Appraisal of Simulations and Observations.* M. E. Schlesinger, Ed., Elsevier, 337–390.